Leukemia
https://doi.org/10.1038/s41375-018-0167-0

ARTICLE

Acute myeloid leukemia

Preclinical evaluation of the selective small-molecule UBA1 inhibitor, TAK-243, in acute myeloid leukemia

Samir H. Barghout[1,2] · Parasvi S. Patel[1,2] · Xiaoming Wang[1] · G. Wei Xu[1] · Simon Kavanagh[1] · Ondrej Halgas[1,3] · Sara F. Zarabi[1,2] · Marcela Gronda[1] · Rose Hurren[1] · Danny V. Jeyaraju[1] · Neil MacLean[1] · Shawn Brennan[4] · Marc L. Hyer[5,9] · Allison Berger[5] · Tary Traore[5] · Michael Milhollen[5] · Adam C. Smith[4,6,7] · Mark D. Minden[1,2] · Emil F. Pai[1,2,3,8] · Razq Hakem[1,2] · Aaron D. Schimmer[1,2]

Received: 28 February 2018 / Revised: 6 April 2018 / Accepted: 2 May 2018

Abstract

Acute myeloid leukemia (AML) is an aggressive hematologic malignancy for which new therapeutic approaches are required. One such potential therapeutic strategy is to target the ubiquitin-like modifier-activating enzyme 1 (UBA1), the initiating enzyme in the ubiquitylation cascade in which proteins are tagged with ubiquitin moieties to regulate their degradation or function. Here, we evaluated TAK-243, a first-in-class UBA1 inhibitor, in preclinical models of AML. In AML cell lines and primary AML samples, TAK-243 induced cell death and inhibited clonogenic growth. In contrast, normal hematopoietic progenitor cells were more resistant. TAK-243 preferentially bound to UBA1 over the related E1 enzymes UBA2, UBA3, and UBA6 in intact AML cells. Inhibition of UBA1 with TAK-243 decreased levels of ubiquitylated proteins, increased markers of proteotoxic stress and DNA damage stress. In vivo, TAK-243 reduced leukemic burden and targeted leukemic stem cells without evidence of toxicity. Finally, we selected populations of AML cells resistant to TAK-243 and identified missense mutations in the adenylation domain of UBA1. Thus, our data demonstrate that TAK-243 targets AML cells and stem cells and support a clinical trial of TAK-243 in this patient population. Moreover, we provide insight into potential mechanisms of acquired resistance to UBA1 inhibitors.

Introduction

Despite improvements in survival rates through the use of targeted agents such as midostaurin and enasidenib [1, 2], relapse rates remain high and > 50% of young adults and 90% of older patients still die from acute myeloid leukemia (AML) [3]. In addition, most patients do not have genetic mutations that are directly druggable [4, 5]. Therefore, it is important to identify novel therapeutic strategies for patients with AML. These new therapies must be active in patients with high-risk molecular and cytogenetic mutations and capable of targeting the leukemic stem cells that are frequently responsible for disease relapse [6].

One such therapeutic approach is to target the ubiquitin-proteasome system (UPS) and particularly the ubiquitin-like modifier-activating enzyme 1 (UBA1) [7]. The UPS is the major cellular machinery responsible for the regulated

Electronic supplementary material The online version of this article (https://doi.org/10.1038/s41375-018-0167-0) contains supplementary material, which is available to authorized users.

✉ Aaron D. Schimmer
aaron.schimmer@utoronto.ca

1 Princess Margaret Cancer Centre, University Health Network, Toronto, ON, Canada

2 Department of Medical Biophysics, Faculty of Medicine, University of Toronto, Toronto, ON, Canada

3 Department of Biochemistry, Faculty of Medicine, University of Toronto, Toronto, ON, Canada

4 Department of Laboratory Medicine, University Health Network, Toronto, ON, Canada

5 Oncology Drug Discovery Unit, Takeda Pharmaceuticals International Co., Cambridge, MA, USA

6 Department of Laboratory Medicine and Pathobiology, Faculty of Medicine, University of Toronto, Toronto, ON, Canada

7 Instituto de Pesquisa Pelé Pequeno Príncipe, Curitiba, Brazil

8 Department of Molecular Genetics, Faculty of Medicine, University of Toronto, Toronto, ON, Canada

9 Agios Pharmaceuticals, Cambridge, MA, USA

Published online: 08 June 2018

degradation of cellular proteins and for maintaining cellular homeostasis [8, 9]. The process of protein degradation via the UPS consists of two major steps: ubiquitylation and proteasomal degradation. Ubiquitylation is a post-translational modification that involves a reversible enzymatic attachment of an 8-kDa, 76 amino acid, evolutionarily conserved polypeptide called ubiquitin to substrate proteins. Ubiquitylation is mediated by the sequential action of members of three enzyme classes: ubiquitin-activating enzymes (E1), ubiquitin-conjugating enzymes (E2), and ubiquitin ligases (E3). UBA1 is the major ubiquitin-activating E1 enzyme and initiates the ubiquitylation cascade [10, 11]. UBA1 adenylates a free ubiquitin molecule to form a ubiquitin–adenylate complex bound to its active adenylation domain [12]. This ubiquitin is then transferred to the catalytic cysteine domain followed by adenylation of another ubiquitin molecule to produce UBA1 loaded with two ubiquitin molecules at two different sites. The loaded UBA1 then interacts with the cognate E2 enzyme to transfer ubiquitin from the catalytic cysteine domain to the active cysteine domain of E2. In concert with E3 enzymes, E2s then transfer ubiquitin to the corresponding protein substrates [12] (Figure S1).

The fate of ubiquitylated proteins depends on the pattern of ubiquitylation. Proteins tagged with a lysine-48 (K48)-linked polyubiquitin chain are recognized and degraded by the proteasome. Through proteasomal degradation, the cell maintains protein homeostasis and degrades excess and misfolded proteins that may adversely affect its survival [13]. Ubiquitylation also affects cellular processes beyond proteasomal protein degradation. For example, ubiquitylation patterns including K63-linked polyubiquitylation and monoubiquitylation constitute non-degradative post-translational modifications that regulate cell signaling [14], DNA repair [15], cell cycle control [16], and endocytosis [17]. Thus, ubiquitylation affects a broad range of non-degradative cellular processes.

Previously, we measured levels of ubiquitylated proteins in lysates from leukemia cell lines and primary AML patient samples as well as normal hematopoietic cells [18]. We showed that levels of UBA1 protein did not differ between AML and normal cells. However, UBA1 was more actively utilized in AML cells and may be a potential therapeutic target for patients with this disease.

TAK-243 is a first-in-class, small-molecule UBA1 inhibitor that bears structural features similar to adenosine sulfamate (Fig. 1a), which acts as a mechanism-based inhibitor of E1 enzymes [8, 19–23]. Here, we evaluated the preclinical efficacy and biological activity of TAK-243 in AML. In addition, we identified two acquired genetic mutations in the adenylation domain of UBA1, which confer resistance to TAK-243.

Materials and methods

Compounds and reagents

TAK-243 (MLN7243) was provided by Takeda Pharmaceuticals. Pevonedistat was provided by Dalton Medicinal Chemistry (Toronto, Canada), Bortezomib and Nelfinavir mesylate were purchased from Selleckchem (Catalog# S1013 and S4282, respectively), Daunorubicin from Sequoia (Catalog# SRP01005d), Mitoxantrone from Sigma-Aldrich (Catalog# M6545), GSK2606414 from Tocris (Catalog# 5107), and 4μ8C from Calbiochem (Catalog# 412512).

Cell lines

OCI-AML2 and K562 cells were cultured in Iscove's modified Dulbecco's medium (IMDM), and NB4 and U937 cells in Roswell Park Memorial Institute (RPMI) medium. Both media were supplemented with 10% fetal bovine serum (FBS) and appropriate antibiotics. Mouse 32D cells were cultured in RPMI medium supplemented with 10% FBS and murine IL-3 from conditioned medium of the mouse X63 cell line (provided as gift from Dr. N. Iscove, University Health Network). TEX cells were cultured in IMDM medium supplemented with 15% FBS, 2 mM L-glutamine, 20 ng/ml recombinant human (rh) stem cell factor (SCF), 2 ng/ml rh-IL-3 and appropriate antibiotics [24]. Cells were not tested for Mycoplasma contamination. U937 and K562 cells were authenticated by STR profiling.

Primary AML and normal hematopoietic cells

Primary human AML cells were obtained from peripheral blood or bone marrow samples isolated from consenting AML patients, with blast count of at least 80% among low-density cells, using Ficoll density gradient centrifugation. Primary normal hematopoietic cells were obtained from healthy consenting volunteers who donated peripheral blood stem cells for allogeneic stem cell transplantation following mobilization by granulocyte-colony stimulating factor (G-CSF). All primary cells were cultured in MyeloCult™ H5100 media (Stem Cell Technologies) supplemented with rh-IL7 (20 ng/ml), rh-IL6 (20 ng/ml), rh-FLT3-L (10 ng/ml), rh-GM-CSF (20 ng/ml), rh-SCF (100 ng/ml), rh-IL-3 (10 ng/ml), and rh-G-CSF (20 ng/ml; Miltenyi). The collection and use of human samples was done based on informed consent from all subjects and approval of the University Health Network Institutional Review Board.

Cytotoxicity assays

CellTiter 96® AQueous MTS Reagent Powder was purchased from Promega (Catalog# G1111), Annexin V-FITC

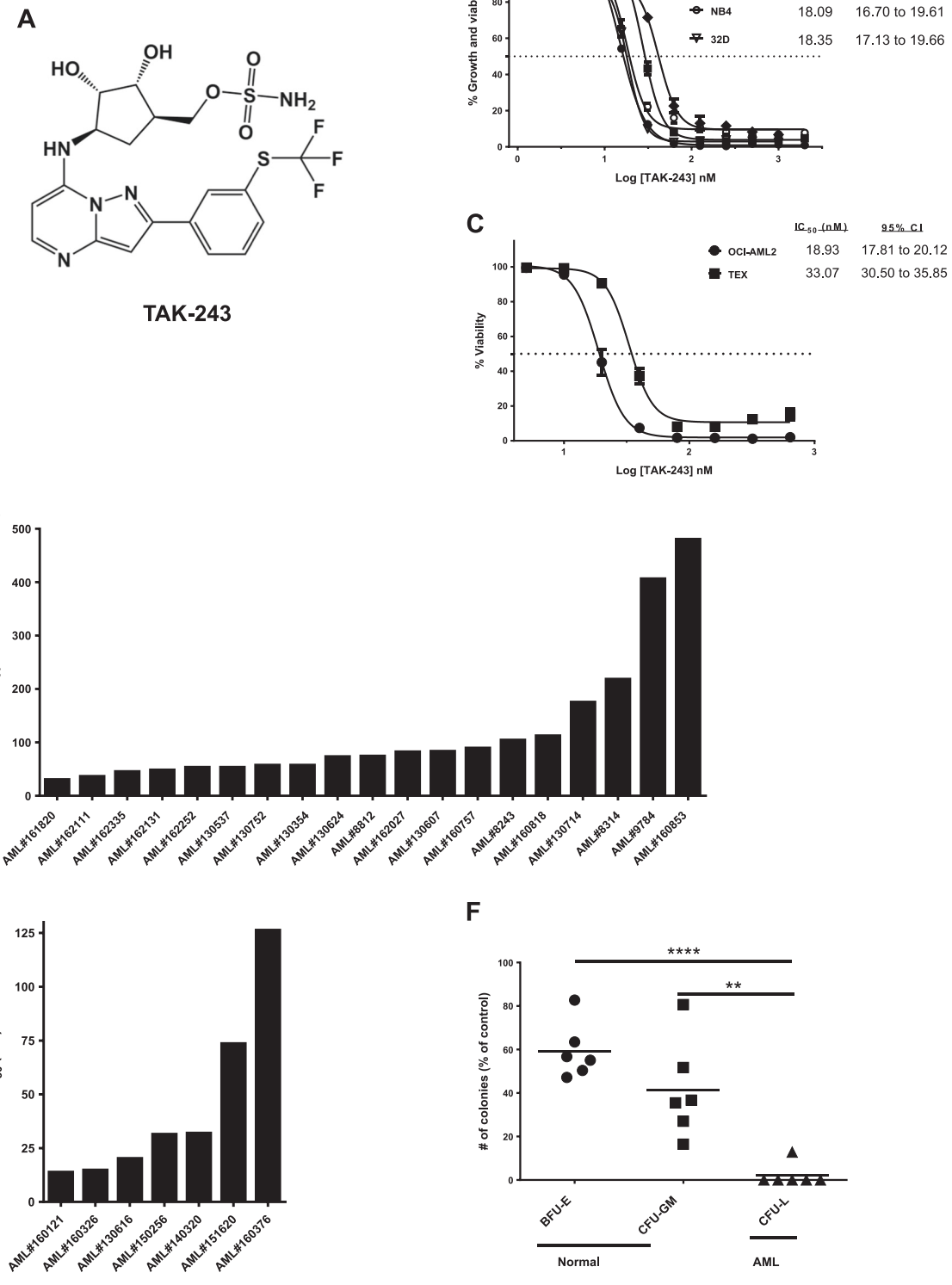
A
TAK-243
B
IC50 (nM)
95% CI
OCI-AML2 15.06 14.23 to 15.94
TEX 27.42 26.06 to 28.84
U937 41.51 38.67 to 44.56
NB4 18.09 16.70 to 19.61
32D 18.35 17.13 to 19.66
% Growth and viability
Log [TAK-243] nM
C
IC50 (nM)
95% CI
OCI-AML2 18.93 17.81 to 20.12
TEX 33.07 30.50 to 35.85
% Viability
Log [TAK-243] nM
D
IC50 (nM)
AML#161820
AML#162111
AML#162335
AML#162131
AML#162252
AML#130537
AML#130752
AML#130354
AML#130624
AML#8812
AML#162027
AML#130607
AML#160757
AML#8243
AML#160818
AML#130714
AML#8314
AML#9784
AML#160853
E
IC50 (nM)
AML#160121
AML#160326
AML#130616
AML#150256
AML#140320
AML#151620
AML#160376
F
# of colonies (% of control)
****
**
BFU-E
CFU-GM
CFU-L
Normal
AML

◀ **Fig. 1** Anti-leukemic activity of TAK-243 in AML cell lines and primary cells. **a** Chemical structure of TAK-243. **b** OCI-AML2, TEX, U937, NB4, and 32D cell lines were treated with increasing concentrations of TAK-243 for 48 h. Cell growth and viability was measured by MTS assay. Insert: the IC_{50} and 95% confidence interval (CI) values (nM) are shown. **c** OCI-AML2 and TEX AML cells were treated with increasing concentrations of TAK-243 for 48 h. Cell viability was measured by Annexin V/PI staining and flow cytometry. All data points in **b** and **c** represent the mean ± SEM of at least three independent experiments. **d** and **e** Primary AML samples were treated with increasing concentrations of TAK-243 for 48 h **d** and 72 h **e**. Cell viability was measured by Annexin V/PI staining ($n = 19$) **d** and cell growth and viability were measured by CellTiter-Fluor ($n = 7$) **e**. The IC_{50} values (nM) were calculated from three technical replicates for each sample and represented on the *Y*-axis with the corresponding sample numbers on the *X*-axis. **f** Primary AML (n = 6) and normal hematopoietic samples ($n = 6$) were treated for 48 h with TAK-243 (250 nM) and then plated into colony-forming assays. Growth of leukemic colonies was measured in the AML cells and burst-forming unit-erythroid (BFU-E) and colony-forming unit-granulocyte, monocyte (CFU-GM) was assessed in the normal hematopoietic cells. The *Y*-axis shows the number of colonies as a percentage of the vehicle-treated controls from individual samples with 2–4 technical replicates per sample. Each data point represents one primary sample and the horizontal lines represent the means of six samples. $^{**}p < 0.01$; $^{****}p < 0.0001$ using one-way ANOVA and Tukey's multiple comparisons test

apoptosis kit from Biovision (Catalog# K101-400), and CellTiter-Fluor kit from Promega (Catalog# G6080). The MTS, Annexin V/propidium iodide (PI), and CellTiter-Fluor assays were conducted as per the manufacturer's guidelines. Flow cytometric analysis of Annexin V/PI-treated samples was performed using BD FACSCANTO flow cytometer (BD Biosciences). Colony formation was assessed by the clonogenic assay as described previously [25]. In brief, primary AML cells (4×10^5 cells) were treated with dimethyl sulfoxide (DMSO) or TAK-243 for 48 h, followed by washing and plating by volume in duplicate in 35 mm dishes (Nunclon, Rochester, USA) to a final volume of 1 ml/dish in MethoCult GF H4434 medium (Stem Cell Technologies, Vancouver, Canada). Cells were then incubated at 37°C, 5% CO_2 with 95% humidity to form colonies. Colonies of at least 10 cells were then counted as previously described [25].

Cellular thermal shift assay (CETSA)

CETSA was conducted as previously described [26]. In brief, OCI-AML2 cells were treated with either DMSO or increasing concentrations of TAK-243 for 30 min. Cells were then washed and re-suspended in phosphate-buffered saline (PBS) containing protease inhibitors (Thermo Fisher Scientific). Cells were then heated to 54°C for 3 min using a thermal cycler to assess the stability of UBA1 and UBA3 and 52°C to assess the stability of UBA6. These temperatures were experimentally derived to produce the optimal thermal shift of the proteins. To assess thermal stability on tumors harvested from TAK-243-treated mice, samples were cut into small pieces and re-suspended in PBS with protease inhibitors followed by heating for 3 min. Cell lysates were then prepared by six freeze–thaw cycles with vigorous vortexing in between, followed by centrifugation twice at 20,000 g for 20 min.

Supplementary methods

Method description for immunoblotting, GRP78 over-expression, immunofluoresence, immunohistochemistry (IHC), animal studies, generation of TAK-243-resistant AML cell lines, detection of *UBA1* mutations and data analysis is available as supplementary information.

Results

TAK-243 induces cell death and decreases clonogenic growth in AML cell lines and primary cells

TAK-243 is a selective UBA1 inhibitor [20]. To determine the effects of TAK-243 on the growth and viability of AML cells, we treated OCI-AML2, TEX, U937, NB4, and 32D cell lines with increasing concentrations of TAK-243. Cell growth and viability were measured with the MTS assay 16 and 48 h after incubation. TAK-243 decreased the growth and viability of AML cell lines in a concentration- and time-dependent manner with a median inhibitory concentration (IC_{50}) values ranging from 20.4 to 83.5 nM after 16 h (Figure S2A) and 15.1 to 41.5 nM after 48 h (Fig. 1b). We confirmed cell death in OCI-AML2 and TEX cells by Annexin V/PI staining and flow cytometry (Fig. 1c and S2B).

We also assessed the effects of TAK-243 in primary AML cells. Primary samples ($n = 19$) were treated with increasing concentrations of TAK-243 for 48 h, and viability measured by Annexin V/PI staining. IC_{50} values ranged from 30 to 480 nM with a median IC_{50} of 74 nM (Fig. 1d). An additional cohort of seven primary samples was treated with TAK-243 for 72 h and growth and viability measured by CellTiter-Fluor assay. IC_{50} values ranged from 13.8 to 126.2 nM with a median IC_{50} of 31.4 nM (Fig. 1e). Sensitivity was not related to morphologic subtype or cytogenetic/molecular mutations as TAK-243 induced cell death in primary AML samples with high-risk cytogenetics, *FLT3* mutations, and samples from patients refractory to induction chemotherapy (Table S3).

Next, we assessed the effects of TAK-243 on clonogenic growth of AML and normal hematopoietic progenitor cells. Primary AML cells ($n = 6$) and normal hematopoietic cells

from consenting individuals donating G-CSF-mobilized peripheral blood stem cells for allotransplants ($n = 6$) were treated with vehicle or TAK-243 for 48 h and then plated into colony-forming assays. TAK-243 nearly abolished the clonogenic growth of all tested primary AML samples, but normal hematopoietic samples were more resistant (Fig. 1f).

TAK-243 preferentially binds to UBA1 in AML cell lines and primary cells

We assessed the binding of TAK-243 to UBA1 in intact cells using CETSA. It is based on the principle of thermal stabilization of proteins upon binding chemical ligands [26]. OCI-AML2 and primary AML cells were treated with TAK-243 at increasing concentrations and the thermal shifts of UBA1, UBA2, UBA3, and UBA6 were measured. In OCI-AML2 cells and primary AML samples, TAK-243 bound UBA1 as evidenced by increased thermostabilization of UBA1 protein with increasing concentrations of TAK-243. In contrast, thermostabilization of UBA3, UBA6, or UBA2 was only observed at much higher concentrations (Fig. 2a, b and S3A-C). As a control, pevonedistat, a selective inhibitor of the related NEDD8-activating enzyme (NAE), preferentially bound the NAE subunit UBA3 over UBA1 as expected (Fig. 2c). Thus, TAK-243 preferentially binds to UBA1 in AML cells and primary samples at concentrations corresponding to its IC_{50}.

TAK-243 reduces ubiquitylation of cellular proteins in AML cells and primary AML samples

UBA1 is the initiating enzyme in the ubiquitylation cascade, so we tested whether UBA1 inhibition by TAK-243 affects ubiquitylation of cellular proteins. OCI-AML2 and 32D cell lines and primary AML samples ($n = 3$) were treated with increasing concentrations of TAK-243. In a time- and concentration-dependent manner, TAK-243 reduced mono- and polyubiquitylation of global cellular proteins in cell lines and primary samples (Fig. 2d–f and S4A). In contrast, TAK-243 inhibited neddylation only at much higher concentrations exceeding those required to induce cell death and at a later time point (Fig. 2g). Taken together, these data highlight the specificity of TAK-243 in reducing global ubiquitylation of proteins.

TAK-243 induces endoplasmic reticulum (ER) stress in AML cells

Failure to degrade misfolded and damaged proteins may cause ER stress and cell death [27, 28]. Given the role of UBA1 as the major ubiquitin-activating enzyme, we tested whether inhibition of UBA1 by TAK-243 induces ER stress and an unfolded protein response (UPR).

Treatment of AML cells with TAK-243 produced changes consistent with increased ER stress. TAK-243 increased $PERK^{Thr981}$ phosphorylation, and induced expression of CHOP and ATF4, indicating activation of the PERK axis of UPR. It also induced $IRE1\alpha^{Ser724}$ phosphorylation, $JNK^{Thr183/Tyr185}$ phosphorylation, and XBP1 splicing to the active form, XBP1s, indicating activation of the IRE1α axis of UPR. Little or no changes were observed in the ATF6 axis or in GRP78 expression levels. Similarly, no changes were observed in UBA1 or UBA6 expression after treatment with TAK-243. Increased ER stress was related to induction of apoptosis as measured by PARP cleavage (Fig. 3a). Of note, no changes were observed in levels of Bcl-2 protein up to 8 h post treatment (Figure S4B).

To investigate the functional importance of ER stress in TAK-243-induced cell death, we assessed the cytotoxicity of TAK-243 after treatment with modulators of protein loading and UPR. First, co-treatment of OCI-AML2 cells with cycloheximide (2.5 μg/ml), a protein synthesis inhibitor that reduces ER loading, abrogated cell death induced by TAK-243 as assessed by annexin V/PI staining after 16 h of incubation (Fig. 3b). Second, we used genetic and chemical approaches to assess the roles of ER stress signaling molecules in mediating cell death by TAK-243. Overexpression of *GRP78*, a repressor of UPR [29], reduced TAK-243 cytotoxicity and apoptosis (Fig. 3c, d). Likewise, co-treatment of OCI-AML2 cells with the PERK inhibitor GSK2606414 [30] increased TAK-243 cytotoxicity, whereas co-treatment with the IRE1α inhibitor 4μ8C [31] rescued TAK-243-mediated cell death (Fig. 3e). In contrast, nelfinavir, an inhibitor of ATF6 activation [32, 33], did not alter cell death consistent with the minimal activation of ATF6 after TAK-243 treatment (Fig. 3a). Taken together, these results show that TAK-243 induces ER stress and activates the PERK and IRE1α arms of UPR, which may, in part, mediate TAK-243 effects.

TAK-243 inhibits the DNA damage response

Apart from proteolytic functions through UPS, ubiquitylation also regulates the DNA damage response [15, 34, 35]. For example, monoubiquitylation of histones H2A and H2B is associated with DNA repair and transcriptional regulation [36, 37]. Therefore, we examined the effects of TAK-243 on DNA damage repair. Treatment of OCI-AML2 cells and primary AML samples ($n = 3$) with TAK-243 decreased H2A and H2B ubiquitylation (Fig. 4a, b, S5A and B).

To determine the effect of TAK-243 on the repair of DNA double-strand breaks (DSBs), we examined OCI-AML2 cells pretreated with TAK-243 or DMSO, for irradiation (IR)-induced foci formation of Ser139 phosphorylated H2AX (γH2AX) and 53BP1, two markers of DSBs [35]. First, we examined γH2AX and 53BP1 foci formation 1 h post IR of OCI-AML2 cells pretreated with DMSO or

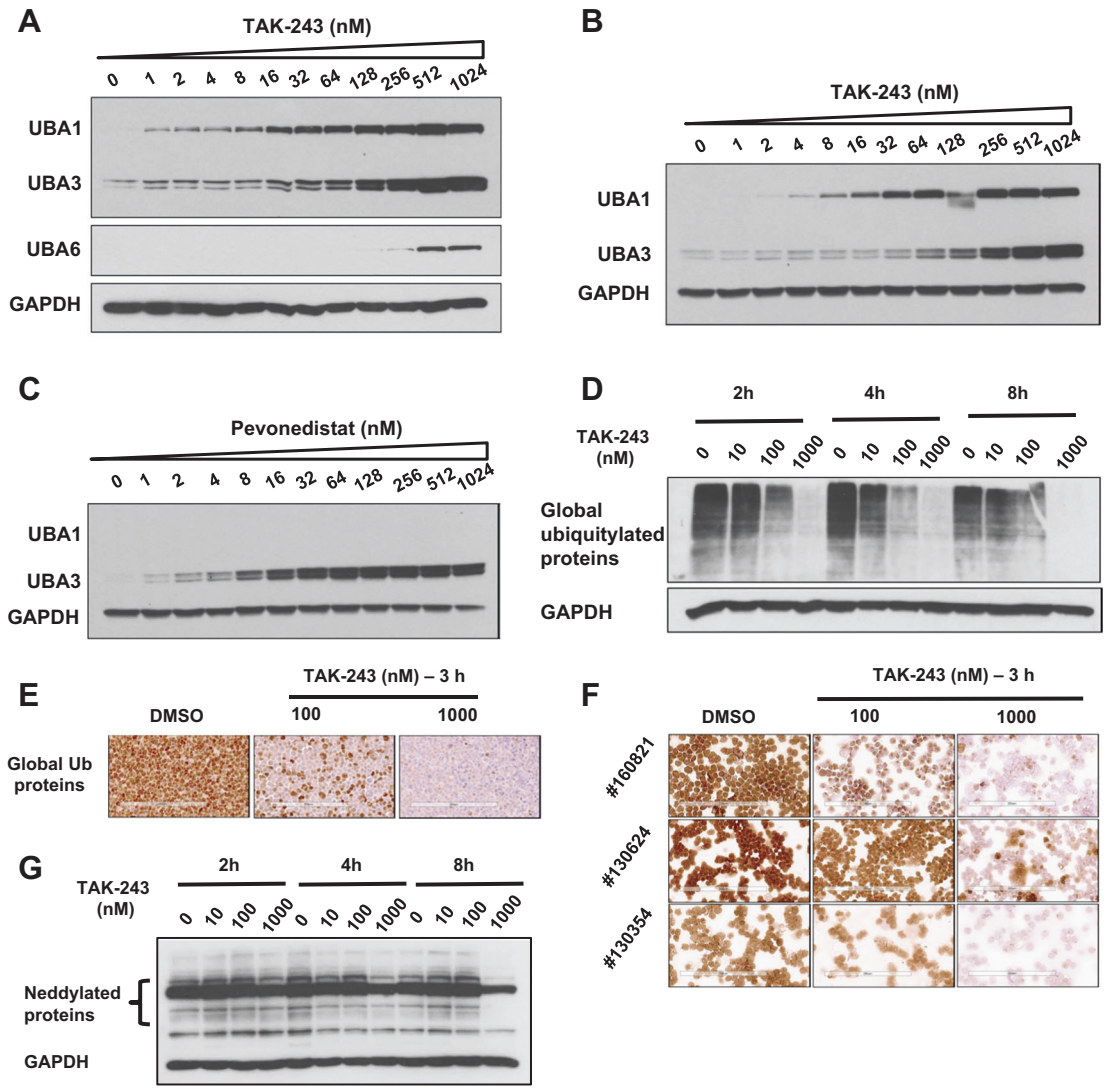

Fig. 2 TAK-243 preferentially binds UBA1 and reduces levels of global protein ubiquitylation in AML cell lines and primary cells. **a** OCI-AML2 cells were treated with increasing concentrations of TAK-243 for 30 min followed by heating the intact cells at 54 °C. After heating, whole-cell lysates were prepared and levels of UBA1, UBA3, UBA6, and GAPDH were measured by immunoblotting. **b** AML patient sample #161820 was treated with increasing concentrations of TAK-243 for 30 min followed by heating the intact cells at 54 °C. After heating, whole cell lysates were prepared and levels of UBA1, UBA3, and GAPDH were measured by immunoblotting. **c** AML patient sample #161820 was treated with increasing concentrations of pevonedistat for 30 min followed by heating the intact cells at 54 °C. After heating, whole cell lysates were prepared and levels of UBA1, UBA3, and GAPDH were measured by immunoblotting. **d** OCI-AML2 cells were treated with increasing concentrations of TAK-243 for increasing times. After treatment, whole cell lysates were prepared and levels of global mono- and poly- ubiquitylated proteins (anti-ubiquitin antibody) and GAPDH were measured by immunoblotting. **e** OCI-AML2 cells were treated with DMSO or TAK-243 (100 and 1000 nM) for 3 h. After treatment, levels of global mono- and poly-ubiquitylated proteins (FK2 antibody) were measured by immunohistochemistry (IHC). Scale bar = 200 µm. **f** Primary AML cells were treated with TAK-243 (100 and 1000 nM) for 3 h. After treatment levels of global mono- and poly-ubiquitylated proteins (FK2 antibody) were measured by IHC. Sample numbers are shown in the figure. Scale bar = 200 µm. **g** OCI-AML2 cells were treated with increasing concentrations of TAK-243 for increasing times. After treatment, whole cell lysates were prepared and levels of neddylated proteins were measured by immunoblotting

TAK-243 for 4 h. Although all samples exhibited similar γH2AX foci formation, recruitment of downstream effector 53BP1 was impaired in cells pretreated with TAK-243, in a concentration-dependent manner, with 1000 nM abolishing all 53BP1 foci formation ($n = 3$) (Fig. 4c, d). Interestingly, OCI-AML2 cells treated with TAK-243 without IR showed increased γH2AX foci, suggesting the ability of TAK-243 to induce DNA damage stress under unirradiated conditions (Figure S5C–E). However, we cannot exclude the possibility that increased γH2AX foci may be secondary to cell death. Furthermore, OCI-AML2 cells pretreated for 2 h with 100 nM of TAK-243 prior to IR, displayed reduced ability to resolve DSBs (γH2AX foci) 24 h post IR. In addition, 24 h post IR, these TAK-243-pretreated cells also exhibited

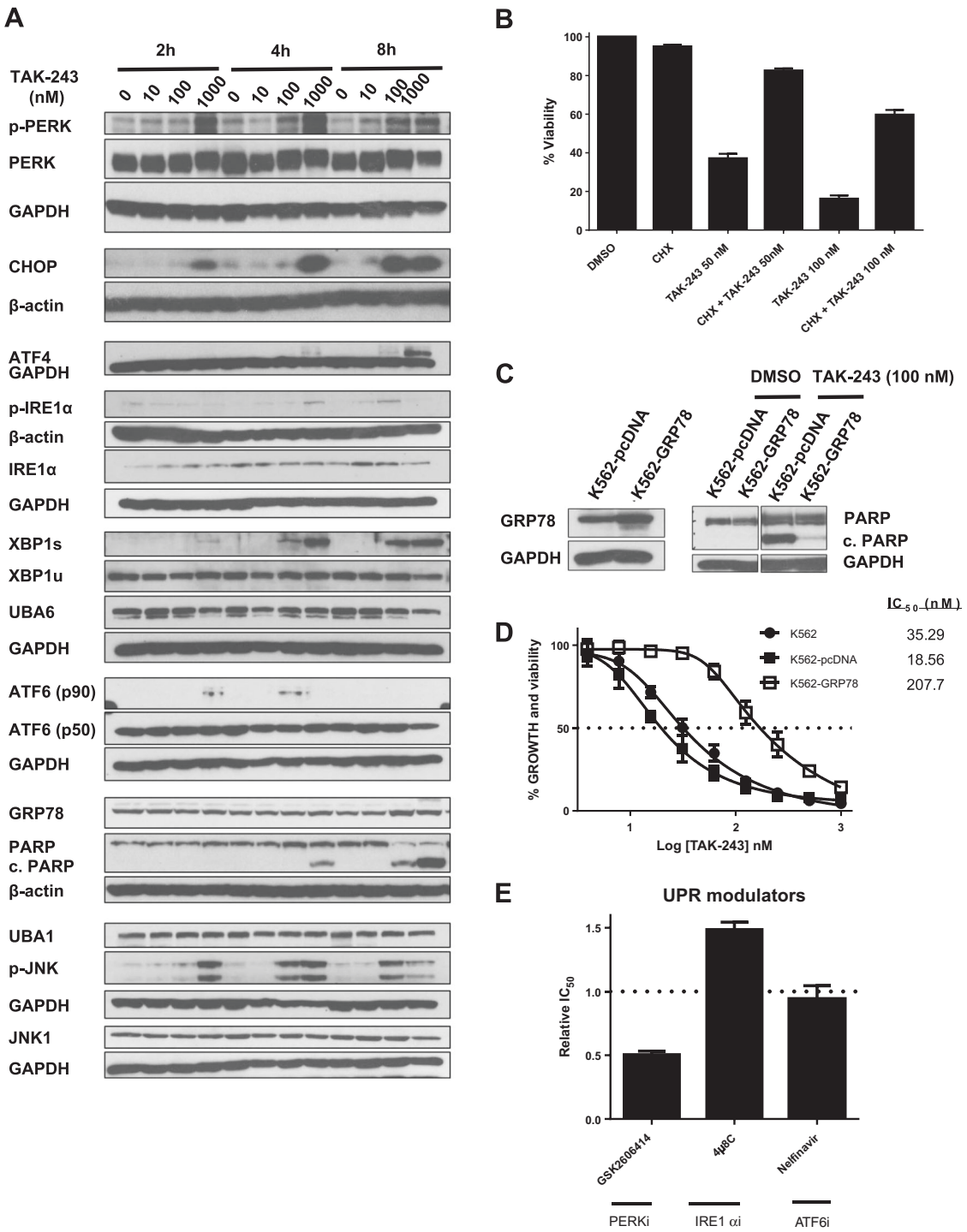

reduced foci formation of 53BP1 compared with DMSO pretreated controls (Fig. 4e, f).

TAK-243 reduces the leukemic burden in a mouse xenograft model of AML

To evaluate the preclinical efficacy and toxicity of TAK-243 in vivo, we used a mouse xenograft model of AML in which OCI-AML2 cells were injected subcutaneously (sc) into the flanks of severe combined immunodeficiency (SCID) mice. After tumors became palpable, mice were treated with either vehicle or TAK-243 at a dose of 20 mg/kg sc twice weekly (BIW). Systemic administration of TAK-243 significantly delayed tumor growth rate and reduced final tumor weights in treated mice as compared with vehicle control (Fig. 5a, b, and S6A). The dose and

◀ **Fig. 3** TAK-243 induces proteotoxic stress in AML cells. **a** OCI-AML2 cells were treated with increasing concentrations of TAK-243 for increasing times. After treatment, whole cell lysates were prepared and levels of UBA1, UBA6, PARP, cleaved PARP (c. PARP) and ER stress related proteins were measured by immunoblotting. GAPDH and β-actin were used as loading controls. **b** OCI-AML2 cells were treated with DMSO, Cycloheximide (CHX; 2.5 μg/ml), TAK-243 (50 nM or 100 nM) or a combination of CHX + TAK-243 for 16 h followed by annexin V/PI staining. Bars represent mean ± SEM of three independent experiments. **c** Left: whole cell lysates of K562 cells overexpressing *GRP78* and their control cells, K562-pcDNA, were prepared and levels of GRP78 were measured by immunoblotting. Right: K562-GRP78 and K562-pcDNA were treated with either DMSO or TAK-243 (100 nM) for 24 h followed by immunoblotting to measure PARP and c. PARP. GAPDH was used as a loading control. **d** Wild-type and transfected K562 cells were treated with increasing concentrations of TAK-243 for 16 h followed by the MTS assay to assess growth and viability. Insert: the IC_{50} values are shown. **e** OCI-AML2 cells were treated with TAK-243 alone or in combination with the UPR modulators GSK2606414 (10 μM), 4μ8C (10 μM), or Nelfinavir (10 μM) for 16 h followed by the MTS assay. The relative IC_{50} compared with TAK-243 alone (considered as 1) are shown. Each bar represents the mean ± SEM of the IC_{50} values calculated from three independent experiments

schedule were well-tolerated with no significant changes in body weight (Fig. S6B). Serum chemistries measured from the blood obtained from mice at the end of treatment showed no increase in levels of total bilirubin, alkaline phosphatase, creatinine, aspartate transaminase, or creatinine kinase between vehicle- and TAK-243-treated mice (Fig. S6C). In addition, no significant changes were observed in gross or histological examination of organs collected at the end of treatment (Fig. S6D).

TAK-243 reduces engraftment of human primary AML cells in the bone marrow of mice

To evaluate the preclinical efficacy of TAK-243 in a more clinically relevant model of AML, primary AML cells were injected into the right femurs of sublethally irradiated NOD-SCID mice. Two weeks after injection of the primary cells, mice were treated with vehicle or TAK-243 (20 mg/kg sc BIW) for 3 weeks. TAK-243 treatment reduced levels of leukemia as assessed by flow cytometric quantification of human $CD45^{+}CD19^{-}CD33^{+}$ cells collected from the non-injected left femurs (Fig. 5c). Secondary transplant experiments demonstrated that TAK-243 also effectively targeted leukemic stem cells in vivo (Fig. 5d).

TAK-243 preferentially targets UBA1 in vivo

We next sought to assess TAK-243 binding to UBA1 and the effects on the ubiquitylation pathway in vivo. Mice with established subcutaneous OCI-AML2 xenograft tumors were treated with vehicle or TAK-243 at a dose of 20 mg/kg sc for two doses. Based on our CETSA data showing that TAK-243 remained bound to UBA1 up to 8 h after washout of the drug from OCI-AML2 cells treated in culture, we killed the mice 8 h after the second dose (Figure S7A). Tumors were collected after killing to assess target engagement of TAK-243. As assessed by CETSA, TAK-243 preferential bound UBA1 over UBA6 in OCI-AML2 tumors (Fig. 5e).

We also examined the effects of TAK-243 on ubiquitylation in tumors and normal tissues after systemic administration to mice. At doses that produce an anti-leukemic effect in vivo, TAK-243 preferentially reduced levels of global ubiquitylated proteins and mono-ubiquitylated H2A and H2B in the leukemic cells compared with normal tissues (Fig. 5f–h and S7B, C and E–I). Finally, TAK-243 preferentially induced caspase 3 cleavage in the leukemic cells compared with normal tissues (Fig. 5g and S7D–I).

Missense mutations in the adenylation domain of *UBA1* confer resistance to TAK-243

To gain insight into potential mechanisms of resistance to TAK-243, we developed TAK-243-resistant cells by two approaches. First, we cultured OCI-AML2 cells continuously in increasing concentrations of TAK-243 starting from the IC_{90} of the drug. We selected a population of TAK-243-resistant cells (OCI-AML2-R_{IC90}) that were 33-fold more resistant to the drug compared with the parental cells (IC_{50} 757 vs 23.4 nM) (Fig. 6a). In the second approach, we cultured cells in a cyclic manner by treating cells with stepwise increasing concentrations of TAK-243 starting from 0.5 nM. We selected a population of TAK-243-resistant cells (OCI-AML2-R_{SW}) that were 28-fold more resistant compared with the parental cells (930.2 vs 33.8 nM) (Fig. 6b). Compared with their parental cell lines, both OCI-AML2-R_{IC90} and OCI-AML2-R_{SW} cells were equally sensitive to pevonedistat, bortezomib, daunorubicin, and mitoxantrone (Fig. S8A–D and S9A–D). Using CETSA, binding of TAK-243 to UBA1 was reduced in both OCI-AML2-R_{IC90} and OCI-AML2-R_{SW}, whereas binding to UBA3 and UBA6 remained unchanged (Fig. 6c, d). Levels of UBA1 did not differ between the parental and resistant cells. Likewise, expression of XBP1s, GRP78 and breast cancer resistance protein was not different in the resistant cells (Fig. S8E and S9E).

To identify the mechanism of resistance to TAK-243, we sequenced the exons spanning the adenylation domain of *UBA1* (exons 12–16 and 23–24) in the resistant cell lines and their parental sensitive cells. We identified different mutations in the two resistant cell lines. In OCI-AML2-R_{IC90} cells, we identified a missense mutation in exon 16 at codon 583 that results in substitution of tyrosine with cysteine (Y583C) (Fig. 6e). In OCI-AML2-R_{SW} cells, we identified a missense mutation in exon 15 at codon 580 that

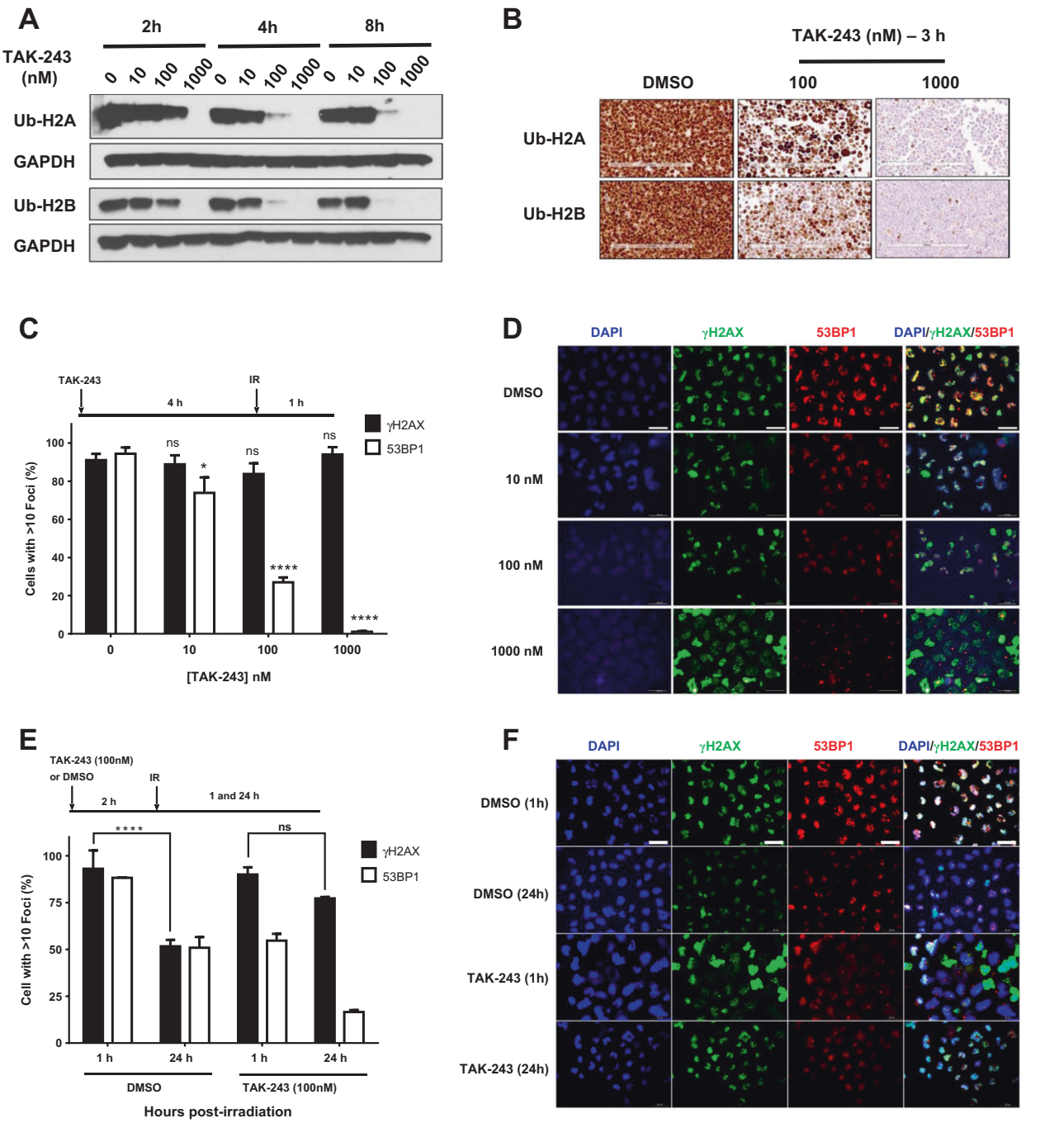

Fig. 4 TAK-243 inhibits DNA double-strand break repair in AML cells. **a**, **b** OCI-AML2 cells were treated with increasing concentrations of TAK-243 for increasing times. After treatment, whole cell lysates were prepared and levels of mono-ubiquitylated histones H2A and H2B were assessed by immunoblotting **a** and immunohistochemistry **b**. Scale bar = 200 µm. **c**, **d** OCI-AML2 cells were treated with increasing concentrations of TAK-243 for 4 h. Cells were then subjected to irradiation (3 Gy) and cytospins were prepared 1 h later. Cells were examined for subnuclear γH2AX and 53BP1 foci by immunofluorescence. Foci were then quantified **c**. Each bar represents mean ± SEM. Representative images of γH2AX and 53BP1 foci are shown **d**. ns: non-significant; $^{*}p \le 0.05$; $^{****}p < 0.0001$ using two-way ANOVA and Sidak's multiple comparisons test. Scale bar = 20 µm. **e**, **f** OCI-AML2 cells were treated with DMSO or TAK-243 (100 nM) for 2 h. Cells were then irradiated (3 Gy) and cytospins were prepared 1 and 24 h post IR. Cells were examined for subnuclear γH2AX and 53BP1 foci by immunofluorescence. Foci were then quantified **e** and bars represent mean ± SEM. Representative images of γH2AX and 53BP1 foci are shown **f**. $^{****}p < 0.0001$ using two-way ANOVA and Sidak's multiple comparisons test

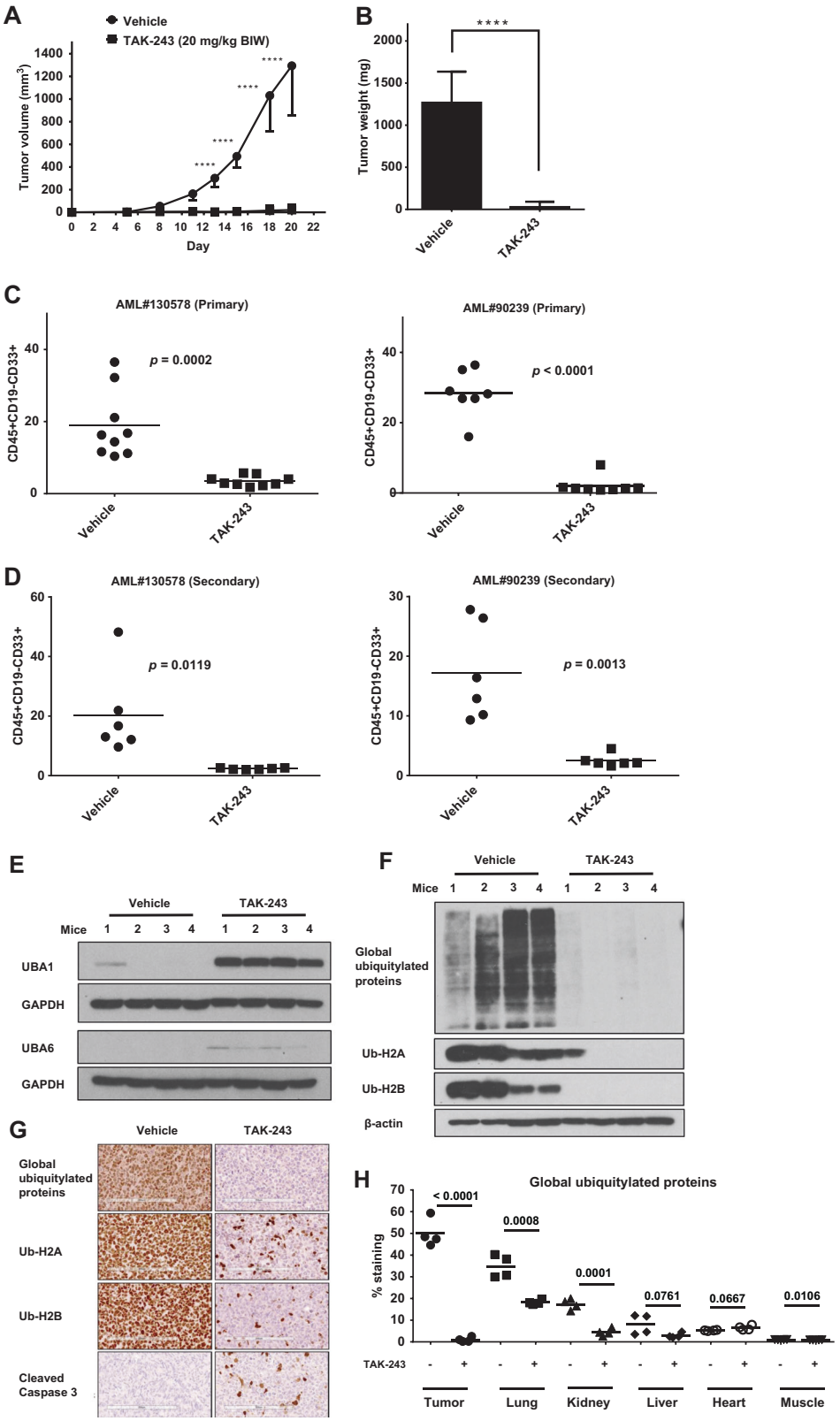
A
Vehicle
TAK-243 (20 mg/kg BIW)
Tumor volume (mm3)
Day
B
Tumor weight (mg)
Vehicle
TAK-243
C
AML#130578 (Primary)
p = 0.0002
AML#90239 (Primary)
p < 0.0001
CD45+CD19-CD33+
D
AML#130578 (Secondary)
p = 0.0119
AML#90239 (Secondary)
p = 0.0013
E
Mice
UBA1
GAPDH
UBA6
F
Global ubiquitylated proteins
Ub-H2A
Ub-H2B
β-actin
G
Cleaved Caspase 3
H
Global ubiquitylated proteins
% staining
Tumor
Lung
Kidney
Liver
Heart
Muscle

◀ **Fig. 5** TAK-243 reduces the leukemic burden in mouse models of AML, and preferentially binds and inhibits UBA1 in AML cells in vivo. **a** OCI-AML2 cells (1×10^6) were injected subcutaneously into the flanks of SCID mice. When the tumors became palpable, mice were randomly divided into two groups ($n = 10$ per group), and treated with vehicle (10 % 2-hydroxypropyl-β-cyclodextrin [HPBCD] in water) or TAK-243 (20 mg/kg) subcutaneously (sc) twice weekly (BIW) for 3 weeks. Tumor volume was assessed by caliper measurements every 2–3 days. $^{****}p < 0.0001$ using repeated-measure two-way ANOVA and Sidak's multiple comparisons test. **b** Tumors were harvested at the end of the study and weighed. The bars represent means ± SD of 10 mice. $^{****}p < 0.0001$ using unpaired *t* test. **c** Two AML patient samples (2.5×10^6 viable trypan blue-negative cells) were injected into the right femurs of NOD-SCID mice that had been sublethally irradiated 24 h previously with 208 rad. Two weeks after injection of the primary cells, mice were treated with TAK-243 (20 mg/kg sc BIW) or vehicle control (10 % HPBCD in water). After 4 weeks of treatment, engraftment of human AML cells into the marrow of the non-injected left femurs was assessed by measuring the percentage of human $CD45^+CD19^-CD33^+$ cells by flow cytometry. **d** Primary human AML cells were isolated from the bone marrow of vehicle- and TAK-243-treated mice in **c**. Equal numbers of viable cells were injected into the right femurs of untreated secondary mice. Mice were killed 5 weeks post injection and engraftment of human cells was assessed by measuring the percentage of human $CD45^+CD19^-CD33^+$ cells by flow cytometry. Each data point in **c** and **d** represents one mouse with the horizontal bars representing the means. Unpaired *t* test was used to determine significance. *p* values and primary sample numbers are shown on the graphs. **e** Mice with established OCI-AML2 tumors were treated with two doses of vehicle or TAK-243 (20 mg/kg) on days 1 and 4. Eight hours after the second dose, mice were killed, and tumors were collected and heated at 54°C followed by lysate preparation. Levels of UBA1, UBA6, and GAPDH were measured by immunoblotting. **f** OCI-AML2 tumors were harvested from mice treated with vehicle or TAK-243 as in **e**. Whole cell lysates were prepared and levels of global ubiquitylated proteins, Ub-H2A, Ub-H2B, and β-actin were measured by immunoblotting. **g**, **h** OCI-AML2 tumors, lungs, kidneys, liver, heart, and muscle were harvested from mice treated with vehicle or TAK-243 as in **e**. Levels of global ubiquitylated proteins, Ub-H2A, Ub-H2B, and cleaved caspase 3 in OCI-AML2 tumors were measured by IHC **g**. Levels of global ubiquitylated proteins in tumors and normal tissues were quantified by taking three random images from different areas of tumors or organs collected from each mouse **h**. The *Y*-axis represents the area of positively stained cells as a percentage of the total area of the image. % staining was quantified by ImageJ software. Four mice were assessed per treatment. Each data point in the graph represents a single mouse and horizontal bars represent the means. Unpaired *t* test was used for determining significance and corresponding *p* values are shown on the graph

results in substitution of alanine with serine (A580S) (Fig. 6f). We confirmed the presence of the mutations by repeating the sequencing in independent cell populations.

Mutations in the highly conserved residue A580 have been reported to confer resistance to TAK-243 using recombinant UBA1 and cell-free enzymatic assays [38]. Therefore, we focused on understanding the potential mechanism by which the Y583C mutation confers resistance to TAK-243. As the structure of human UBA1 has not been reported yet, we used recently published structure of highly homologous yeast Uba1 (ScUba1) in complex with the drug [38] to model the interactions of TAK-243 with the Y583C human UBA1 (HsUBA1) mutant (Fig. S8F).

Unlike much of the protein, the 583 position is not well conserved in the E1 family of enzymes. However, it is usually occupied by larger side chains of tyrosine (ScUba1, HsUBA1, 6, 7), tryptophan (HsUBA3), or histidine (HsUBA2). Introducing cysteine into this position likely perturbs the hydrophobic core and creates a cavity between C583 and its neighboring residues. Moreover, it also eliminates putative hydrogen bonds that Y583 of human UBA1 can form with G553 and E557 (G521 and E525 in ScUba1; Fig. S8F). Thus, the Y583C mutation likely destabilizes this side of the binding pocket and may prevent efficient binding of the thio(trifluoromethyl) hook of TAK-243 to HsUBA1 surface.

Discussion

In this study, we evaluated the UBA1 inhibitor TAK-243 in AML. By the CETSA assay, TAK-243 preferentially bound UBA1 in AML cell lines and primary AML samples over the related E1 enzymes UBA2, UBA3, and UBA6. Moreover, TAK-243 preferentially inhibited UBA1-mediated ubiquitylation in AML over the activity of the other E1 enzymes. Thus, these data support biochemical studies demonstrating TAK-243 as a preferential UBA1 inhibitor [20]. TAK-243 inhibits UBA1 by a mechanism referred to as substrate-assisted inhibition, a unique mechanism that imparts potency and selectivity to members of this class [19, 20]. As such, it is similar to pevonedistat that binds UBA3 and acts as a selective mechanism-based inhibitor of neddylation [21, 22].

Our studies in vitro and in vivo demonstrated that TAK-243 preferentially targeted AML cells and stem/progenitors over normal cells and normal hematopoietic progenitors. Moreover, TAK-243 preferentially inhibited ubiquitylation in AML cells over normal cells in vivo. These data are consistent with our previous studies demonstrating that UBA1 enzymes have reduced reserve capacity in AML compared with normal hematopoietic cells [18]. In addition, these data help explain the therapeutic window we observed with TAK-243 in our mouse models of leukemia. Hyer et al. [20] evaluated the pharmacokinetics of TAK-243 in mice and reported that a maximal plasma concentration of 2.69 μM was achieved after a dose of 18.8 mg/kg. Future clinical studies in AML will be necessary to determine anti-leukemic concentrations of TAK-243 that can be obtained in humans and to define the efficacy and toxicity of this drug in patients with AML.

TAK-243 induced ER stress in AML cells. van Galen et al. [39] reported that hematopoietic stem cells are more sensitive to ER stress stimuli compared with more

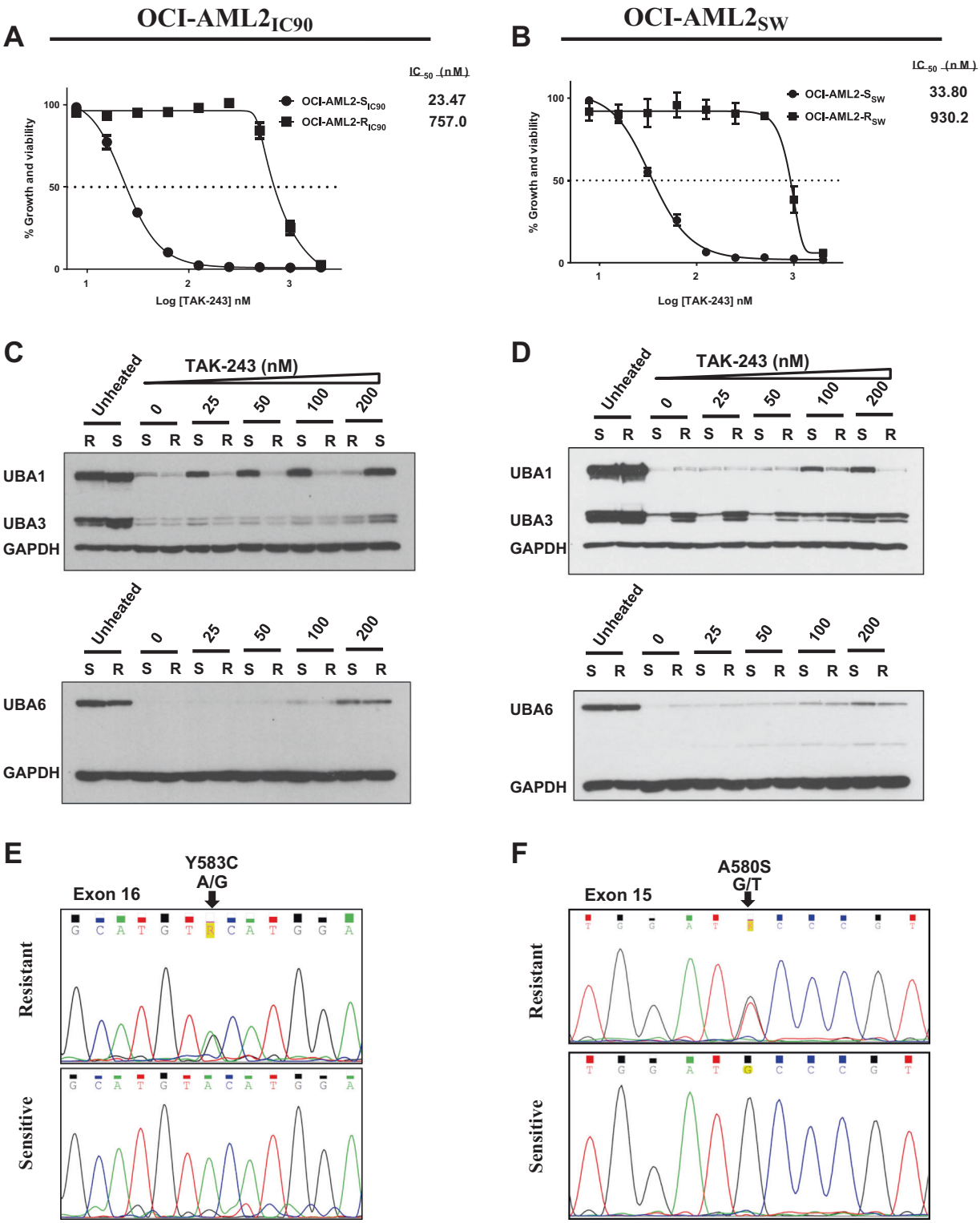

differentiated cells. Therefore, the activity of TAK-243 against leukemic stem and progenitor cells may derive in part from its ability to induce ER stress and an increased sensitivity of leukemic stem cells to ER stressors.

Ubiquitylation is critical for DNA damage response [35]. Indeed, several proteins must be ubiquitylated for efficient DSB repair. For instance, ubiquitylation of H2A-type histones and Histone H1 at DSB-flanking sites triggers

◀ **Fig. 6** Y583C and A580S *UBA1* mutations confer resistance to TAK-243 in AML cells. **a**, **b** Sensitive and resistant OCI-AML2$_{IC90}$ and OCI-AML2$_{SW}$ cell lines were treated with increasing concentrations of TAK-243 for 48 h. After treatment, cell growth and viability were measured by the MTS assay. Insert: IC_{50} values of the parental and resistant cells. **c**, **d** Sensitive (S) and resistant (R) OCI-AML2$_{IC90}$ and OCI-AML2$_{SW}$ cell lines were treated with increasing concentrations of TAK-243 for 30 min. For CETSA, cells were heated to 54°C followed by lysate preparation. Lysates of unheated controls were prepared in parallel. Levels of UBA1, UBA3, UBA6 and GAPDH were then determined by immunoblotting. **e**, **f** Sanger sequencing chromatograms showing Y583C and A580S missense mutations of *UBA1* in OCI-AML2$_{IC90}$ and OCI-AML2$_{SW}$ cell lines. Corresponding *UBA1* exons are shown in the figure. Y583C: substitution of tyrosine with cysteine at *UBA1* codon 583; A580S: substitution of alanine with serine at *UBA1* codon 580

orchestrated recruitment to these damage sites of a number of DSB signaling and repair proteins including 53BP1 and BRCA1; thus, allowing the repair through non-homologous end-joining (NHEJ) and homologous recombination, respectively. Our data indicate that TAK-243 restrains levels of Ub-H2A and Ub-H2B and impairs DSB repair. Notably, the recruitment of 53BP1 and its retention at DSB-flanking sites was significantly impaired. Given the importance of 53BP1 for NHEJ, the impaired IR-induced 53BP1 foci formation after TAK-243 treatment suggests that TAK-243 impairs NHEJ efficiency and this likely contributes to impaired DSB repair.

Several classes of proteins are known to be regulated by ubiquitylation such as nuclear factor (NF)-κB, cell cycle proteins (e.g., cyclins and CDK inhibitors), and short-lived proapoptotic proteins (e.g., p53) [8, 40]. Ubiquitylation is also involved in regulating DNA damage response (e.g., double-strand break repair, translesion synthesis, and Fanconi anemia pathway) [15]. In the context of AML, a number of these proteins play important biological roles and their perturbation by UBA1 inhibition may account for the observed cytotoxicity. For example, NF-κB was reported to be constitutively active in AML and in leukemic stem cells compared with normal progenitors [41, 42]. This higher activity is maintained by proteasomal degradation of the NF-κB inhibitor IκBα, which may explain the higher requirement of UBA1 and the observed therapeutic window in AML. Although UBA1 inhibition is expected to stabilize p53, proteasomal inhibition was reported to be efficacious in AML cells independent of p53 status [43].

To understand potential mechanisms of resistance to TAK-243, we selected a population of resistant cells and identified Y583C and A580S missense mutations in the adenylation domain of UBA1. Based on our analysis of available E1 enzyme structures, resistance of the Y583C mutant is likely caused by elimination of hydrogen bonds and destabilization of the protein hydrophobic core. Only further structural studies will be able to fully explain the mechanism of resistance of Y583C and A580S mutants to TAK-243. Of note, Y583 in human UBA1 corresponds to Y551 in yeast Uba1, which was reported to be uniquely involved in binding TAK-243 but not pevonedistat or ABPA3, a dual inhibitor of UBA1 and NAE [38, 44]. On the other hand, mutation in A580 has been reported to confer TAK-243 resistance in recombinant UBA1 [38]. In addition, A580 corresponds to A171 in NAE, which was also involved in pevonedistat resistance [45, 46]. Thus, we report for the first time Y583C mutation as a TAK-243-specific resistance mechanism in a cell-based model, which may have clinical relevance in AML and potentially other malignancies.

In summary, our study demonstrates TAK-243 is a selective UBA1 inhibitor with a potent anti-leukemic activity in cell-based and animal models of AML. It decreases the abundance of ubiquitylated proteins, induces proteotoxic stress, and inhibits DNA repair in AML. In addition, TAK-243 exhibits preferential activity toward leukemic versus normal progenitors in vitro and inhibits primary and secondary engraftment of patient-derived leukemic cells in bone marrow of mice confirming its activity towards leukemic stem and progenitor cells. It also displays preferential inhibition of UBA1 in tumor xenografts over normal tissues, explaining in part its tolerability in mice. Our study also reports missense mutations in *UBA1* that confer acquired resistance to TAK-243 and may have clinical relevance. In conclusion, our findings reveal preclinical efficacy and tolerability of TAK-243 and support advancement of this drug to a phase 1 clinical trial in AML.

Acknowledgements We thank Dr. James Brownell from Takeda Pharmaceuticals for critical review of the biochemical aspects of the manuscript, and Dr. Michael Sintchak for invaluable scientific advice. We also thank Jill Flewelling and Francesca Pulice at Princess Margaret Cancer Centre for administrative assistance. This work was supported by a research grant from Takeda Pharmaceuticals Inc., the Princess Margaret Cancer Centre Foundation, Canadian Institutes of Health Research (CIHR), the Ontario Institute of Cancer Research, the Canada Research Chairs program, The Ontario Ministry of Research and Innovation, and The Ministry of Long Term Health and Planning in the Province of Ontario. A.D.S. holds the Barbara Baker Chair in Leukemia and Related Diseases. S.H.B. is supported by Ontario Trillium Scholarship, Department of Medical Biophysics fellowship and GSEF scholarship from the Faculty of Medicine, University of Toronto. IHC staining was done in the Applied Molecular Profiling Laboratory (AMPL) facility and imaging was done in the Advanced Optical Microscopy Facility (AOMF) at Princess Margaret Cancer Centre.

Conflict of interest A.D.S. received research funding from Takeda Pharmaceutical Company Limited. A.B., T.T., and M.M. are employees of Takeda Pharmaceutical Company Limited, and M.L.H. was employed by Takeda Pharmaceutical Company Limited at the time of the study.

References

1. Stone RM, Mandrekar SJ, Sanford BL, Laumann K, Geyer S, Bloomfield CD, et al. Midostaurin plus chemotherapy for acute myeloid leukemia with a FLT3 mutation. N Engl J Med. 2017;377:454–64.
2. Mitch Leslie, Positive first trial of enasidenib for AML. *Cancer Discov.* 2017; **7**: OF1.
3. Ferrara F, Schiffer CA. Acute myeloid leukaemia in adults. Lancet. 2013;381:484–95.
4. Dohner H, Weisdorf DJ, Bloomfield CD. Acute myeloid leukemia. N Engl J Med. 2015;373:1136–52.
5. Khwaja A, Bjorkholm M, Gale RE, Levine RL, Jordan CT, Ehninger G, et al. Acute myeloid leukaemia. Nat Rev Dis Prim. 2016;2:16010.
6. Shlush LI, Mitchell A, Heisler L, Abelson S, Ng SWK, Trotman-Grant A, et al. Tracing the origins of relapse in acute myeloid leukaemia to stem cells. *Nature*. 2017;547:104–08.
7. Hoeller D, Dikic I. Targeting the ubiquitin system in cancer therapy. Nature. 2009;458:438–44.
8. Bedford L, Lowe J, Dick LR, Mayer RJ, Brownell JE. Ubiquitin-like protein conjugation and the ubiquitin-proteasome system as drug targets. Nat Rev Drug Discov. 2011;10:29–46.
9. Hoeller D, Hecker CM, Dikic I. Ubiquitin and ubiquitin-like proteins in cancer pathogenesis. Nat Rev Cancer. 2006;6:776–88.
10. Clague MJ, Heride C, Urbe S. The demographics of the ubiquitin system. Trends Cell Biol. 2015;25:417–26.
11. Groen EJ, Gillingwater TH. UBA1: at the crossroads of ubiquitin homeostasis and neurodegeneration. Trends Mol Med. 2015;21:622–32.
12. Schulman BA, Harper JW. Ubiquitin-like protein activation by E1 enzymes: the apex for downstream signalling pathways. Nat Rev Mol Cell Biol. 2009;10:319–31.
13. Brodsky JL. Cleaning up: ER-associated degradation to the rescue. Cell. 2012;151:1163–7.
14. Chen ZJ, Sun LJ. Nonproteolytic functions of ubiquitin in cell signaling. Mol Cell. 2009;33:275–86.
15. Ulrich HD, Walden H. Ubiquitin signalling in DNA replication and repair. Nat Rev Mol Cell Biol. 2010;11:479–89.
16. Nakayama KI, Nakayama K. Ubiquitin ligases: cell-cycle control and cancer. Nat Rev Cancer. 2006;6:369–81.
17. Clague MJ, Liu H, Urbe S. Governance of endocytic trafficking and signaling by reversible ubiquitylation. Dev Cell. 2012;23:457–67.
18. Xu GW, Ali M, Wood TE, Wong D, Maclean N, Wang X, et al. The ubiquitin-activating enzyme E1 as a therapeutic target for the treatment of leukemia and multiple myeloma. Blood. 2010;115:2251–9.
19. Chen JJ, Tsu CA, Gavin JM, Milhollen MA, Bruzzese FJ, Mallender WD, et al. Mechanistic studies of substrate-assisted inhibition of ubiquitin-activating enzyme by adenosine sulfamate analogues. J Biol Chem. 2011;286:40867–77.
20. Hyer ML, Milhollen MA, Ciavarri J, Fleming P, Traore T, Sappal D, et al. A small-molecule inhibitor of the ubiquitin activating enzyme for cancer treatment. *Nat Med* 2018;24:186–93.
21. Brownell JE, Sintchak MD, Gavin JM, Liao H, Bruzzese FJ, Bump NJ, et al. Substrate-assisted inhibition of ubiquitin-like protein-activating enzymes: the NEDD8 E1 inhibitor MLN4924 forms a NEDD8-AMP mimetic in situ. Mol Cell. 2010;37:102–11.
22. Soucy TA, Smith PG, Milhollen MA, Berger AJ, Gavin JM, Adhikari S, et al. An inhibitor of NEDD8-activating enzyme as a new approach to treat cancer. Nature. 2009;458:732–6.
23. Ciavarri J, Langston S. 8.04 - The Discovery of First-in-Class Inhibitors of the Nedd8-Activating Enzyme (NAE) and the Ubiquitin-Activating Enzyme (UAE). In: Rotella D, Ward SE, (eds). Comprehensive Medicinal Chemistry III.. Oxford: Elsevier; 2017. pp. 95–112.
24. Warner JK, Wang JC, Takenaka K, Doulatov S, McKenzie JL, Harrington L, et al. Direct evidence for cooperating genetic events in the leukemic transformation of normal human hematopoietic cells. Leukemia. 2005;19:1794–805.
25. Spagnuolo PA, Hu J, Hurren R, Wang X, Gronda M, Sukhai MA, et al. The antihelmintic flubendazole inhibits microtubule function through a mechanism distinct from Vinca alkaloids and displays preclinical activity in leukemia and myeloma. Blood. 2010;115:4824–33.
26. Jafari R, Almqvist H, Axelsson H, Ignatushchenko M, Lundback T, Nordlund P, et al. The cellular thermal shift assay for evaluating drug target interactions in cells. Nat Protoc. 2014;9:2100–22.
27. Christianson JC, Ye Y. Cleaning up in the endoplasmic reticulum: ubiquitin in charge. Nat Struct Mol Biol. 2014;21:325–35.
28. Smith MH, Ploegh HL, Weissman JS. Road to ruin: targeting proteins for degradation in the endoplasmic reticulum. Science. 2011;334:1086–90.
29. Wang CY, Guo ST, Wang JY, Liu F, Zhang YY, Yari H, et al. Inhibition of HSP90 by AUY922 preferentially kills mutant KRAS colon cancer cells by activating Bim through ER stress. Mol Cancer Ther. 2016;15:448–59.
30. Moreno JA, Halliday M, Molloy C, Radford H, Verity N, Axten JM, et al. Oral treatment targeting the unfolded protein response prevents neurodegeneration and clinical disease in prion-infected mice. Sci Transl Med. 2013;5:206ra138.
31. Cross BC, Bond PJ, Sadowski PG, Jha BK, Zak J, Goodman JM, et al. The molecular basis for selective inhibition of unconventional mRNA splicing by an IRE1-binding small molecule. Proc Natl Acad Sci USA. 2012;109:E869–878.
32. Guan M, Su L, Yuan YC, Li H, Chow WA. Nelfinavir and nelfinavir analogs block site-2 protease cleavage to inhibit castration-resistant prostate cancer. Sci Rep. 2015;5:9698.
33. Guan M, Fousek K, Chow WA. Nelfinavir inhibits regulated intramembrane proteolysis of sterol regulatory element binding protein-1 and activating transcription factor 6 in castration-resistant prostate cancer. FEBS J. 2012;279:2399–411.
34. Al-Hakim A, Escribano-Diaz C, Landry MC, O'Donnell L, Panier S, Szilard RK, et al. The ubiquitous role of ubiquitin in the DNA damage response. DNA Repair (Amst). 2010;9:1229–40.
35. Schwertman P, Bekker-Jensen S, Mailand N. Regulation of DNA double-strand break repair by ubiquitin and ubiquitin-like modifiers. Nat Rev Mol Cell Biol. 2016;17:379–94.
36. Weake VM, Workman JL. Histone ubiquitination: triggering gene activity. Mol Cell. 2008;29:653–63.
37. Uckelmann M, Sixma TK. Histone ubiquitination in the DNA damage response. DNA Repair. 2017;56:92–101.
38. Misra M, Kuhn M, Lobel M, An H, Statsyuk AV, Sotriffer C, et al. Dissecting the specificity of adenosyl sulfamate inhibitors targeting the ubiquitin-activating enzyme. *Structure*. 2017;25:1120–29.
39. van Galen P, Kreso A, Mbong N, Kent DG, Fitzmaurice T, Chambers JE, et al. The unfolded protein response governs integrity of the haematopoietic stem cell pool during stress. Nature. 2014;510:268–72.
40. Yang Y, Kitagaki J, Dai RM, Tsai YC, Lorick KL, Ludwig RL, et al. Inhibitors of ubiquitin-activating enzyme (E1), a new class of potential cancer therapeutics. Cancer Res. 2007;67:9472–81.
41. Bosman MC, Schuringa JJ, Vellenga E. Constitutive NF-kappaB activation in AML: causes and treatment strategies. Crit Rev Oncol Hematol. 2016;98:35–44.

42. Guzman ML, Neering SJ, Upchurch D, Grimes B, Howard DS, Rizzieri DA, et al. Nuclear factor-kappaB is constitutively activated in primitive human acute myelogenous leukemia cells. Blood. 2001;98:2301–7.
43. Csizmar CM, Kim DH, Sachs Z. The role of the proteasome in AML. Blood Cancer J. 2016;6:e503.
44. An H, Statsyuk AV. An inhibitor of ubiquitin conjugation and aggresome formation. Chem Sci. 2015;6:5235–45.
45. Milhollen MA, Thomas MP, Narayanan U, Traore T, Riceberg J, Amidon BS, et al. Treatment-emergent mutations in NAEbeta confer resistance to the NEDD8-activating enzyme inhibitor MLN4924. Cancer Cell. 2012;21:388–401.
46. Toth JI, Yang L, Dahl R, Petroski MD. A gatekeeper residue for NEDD8-activating enzyme inhibition by MLN4924. Cell Rep. 2012;1:309–16.